JOURNAL OF STRUCTURAL BIOLOGY **116,** 399–412 (1996)
ARTICLE NO. 0057

Molecular and Supramolecular Architecture of the *Salmo gairdneri* Proteinaceous Eggshell during Development

PARASKEVI PAPADOPOULOU

Department of Biochemistry, Cell and Molecular Biology, and Genetics, University of Athens, Athens 15701, Greece

VASSILIS K. GALANOPOULOS

Department of Biology, University of Crete, and Institute of Molecular Biology and Biotechnology, Iraklion 71110, Crete, Greece

AND

STAVROS J. HAMODRAKAS

Department of Biochemistry, Cell and Molecular Biology, and Genetics, University of Athens, Athens 15701, Greece

Received November 27, 1995, and in revised form January 11, 1996

A detailed developmental study of eggshell architecture of the fish *Salmo gairdneri* (rainbow trout) was performed using transmission and scanning electron microscopy. Thioglycollic acid treatment and freeze-fracturing reveal that fibrils ca. 5–10 nm in diameter constitute each lamella of the helicoidal eggshell. Freeze-fracturing also permits a direct visualization of the helicoidal architecture. Laser-Raman studies of the eggshell indicate abundant antiparallel β-pleated-sheet conformation in the eggshell proteins of *S. gairdneri* during all developmental stages. Apparently, this conformation dictates formation of the helicoidal structure. Disulfide bonds, together with isopeptide bonds, cross-link *S. gairdneri* eggshell proteins throughout development.

INTRODUCTION

Several extracellular fibrous structures, frequently proteinaceous, are known to have helicoidal architecture, a biological analogue of a cholesteric liquid crystal. Such architecture is found in plant cell walls, arthropod cuticles, vertebrate tendons, and insect and fish eggshells (Hamodrakas, 1992; Mazur *et al.,* 1982; Bouligand, 1972). It consists of helicoidally arranged parallel planes or sheets of fibrils. Within individual planes the fibrils are oriented parallel to each other. Between successive planes the fibril direction rotates progressively, thus giving rise to a helix, with its axis perpendicular to the planes. A helicoidal organization is identified ultrastructurally, usually under a transmission electron microscope, as a lamellar structure, exhibiting in suitably cut, oblique thin sections, parabolic arrays of fibrils ("arced" patterns), which constitute each lamella (Bouligand, 1972).

From observations on the silkmoth eggshell we proposed the twisted antiparallel β-pleated sheet as the protein molecular conformation which dictates the formation of helicoidal architecture in proteinaceous eggshells (Hamodrakas, 1984, 1992, and references therein). Our proposal was confirmed in the proteinaceous lepidopteran eggshells of *Manduca sexta* and *Sesamia nonagrioides* (Orfanidou *et al.,* 1993, 1995) and also in mature fish eggshells of *Salmo gairdneri* (Hamodrakas et al., 1987).

It is of interest to know whether the helicoidal structures found in such diverse proteinaceous systems share an underlying molecular conformation and how, and if, this conformation influences the morphogenesis of the resulting structures, most probably by self-assembly mechanisms. In this report, we present results obtained from studies of all pre- and postovulatory stages of development of the trout *S. gairdneri* eggshell utilizing transmission and scanning electron microscopy and freeze-fracturing, which show its structural changes during choriogenesis (eggshell development). Based on the developmental stages of oogenesis determined by previous investigators (Yamamoto *et al.,* 1965; van den Hurk and Peute, 1979) a step by step formation of the eggshell was examined and a set of corresponding stages for choriogenesis was defined. Special attention was given to the study of the la-

1047-8477/96 $18.00

mellar helicoidal architecture and fibrillar ultrastructure of mature eggshells.

Furthermore, the secondary structure of *S. gairdneri* eggshell proteins and side-chain environment were studied at different developmental stages utilizing laser-Raman spectroscopy.

MATERIALS AND METHODS

Experiments were carried out on eggs of the rainbow trout *S. gairdneri* at pre- and postovulatory stages. Rainbow trout eggs were obtained from fresh individuals from the fish farm of river Louros, supervised by the Greek Ministry of Agriculture. Samples were taken on a monthly basis from a synchronized population of fish for a 1-year period (January to December 1987).

Terms Used

To minimize confusion associated with the variable nomenclature used to describe the eggshell of teleost fish eggs (for commonly used terms see the reviews of Hurley and Fisher, 1966; Anderson, 1967; Laale, 1980) the terms used in this study to describe the different layers within the eggshell are: cortex radiatus externus (CRE), cortex radiatus internus (CRI), and cortex radiatus subinternus (CRS). CRE refers to the thin osmiophilic ("electron-dense") outermost layer, CRI refers to the thick proteinaceous inner layer, and CRS to the innermost layer apparent in some teleost species (see also Flugel, 1964a,b, 1967; Grierson and Neville, 1981; Groot and Alderdice, 1984). Hereafter, the terms eggshell and chorion will be used interchangeably. This is not strictly correct since in several systems the eggshell consists of chorion and vitelline membrane.

Electron Microscopy

Samples of whole eggs and isolated eggshells at pre- and postovulatory stages, prepared following normal procedures, were examined under a JEOL 100C and a Philips EM200 transmission electron microscopes operating at 100 and 60 kV, respectively, and under a JEOL-840 scanning electron microscope operating at 10 kV.

Eggshells were either isolated from the egg proper or left intact and were fixed in 2% glutaraldehyde and 2% paraformaldehyde in 0.08 *M* sodium cacodylate buffer. After washing in 4% sucrose in 0.08 *M* sodium cacodylate buffer, the samples were fixed in 2% OsO_4 in distilled water at 4°C for 1 hr. Postfixed samples were dehydrated in a graded series of ethanol solutions.

For transmission electron microscopy, samples were further treated with propylene oxide and embedded in Epon 812–Araldite–dodecenyl succinic anhydrite (25:20:60 g) resin. A Sorval MT2 ultramicrotome was used to obtain thin sections. To observe microfibrils of the proteinaceous eggshell, the glutaraldehyde fixation was omitted. Instead, eggshells were pretreated with 0.5 *M* thioglycollic acid at pH 5.5 for 24 hr, following the method of Filshie and Rogers (1962). This method has been used to resolve fine structure in feather keratin and has also been employed by Grierson and Neville (1981) to resolve microfibrillar ultrastructure in the cod *Gadus morrhua* eggshell: A large number of disulfide cross-links hinder stain penetration into sections. Thioglycollic acid has the effect of breaking disulfide bonds and the resultant sulfydryl groups become available for staining with osmium second lead hydroxide. Microfibrils could not be resolved in eggshells using uranyl acetate or potassium permanganate as stains and, therefore, since our early preparations did not resolve microfibrillar ultrastructure, thioglycollic acid treatment was tried. In some cases, eggshells were pretreated with 6 *M* urea, followed by 1% β-mercaptoethanol for 24 hr to remove the outer osmiophilic layer of the eggshell CRE and reveal the arrangement of the pore canals on the outer surface of the eggshell before continuing with fixation.

For scanning electron microscopy, the dehydrated samples were processed for critical point drying in a Tousimis 780A critical point dryer. Sections of dehydrated and dried samples were mounted on copper stubs, with either a double-sided adhesive tape or silver paste. Secured to the stubs, the samples were coated with gold/palladium in a sputter coater with a 18-nm coat. All dried preparations were stored in a vacuum desiccator at room temperature.

Cross sections of the eggshells were obtained by several techniques. Fresh unfixed eggshells were either torn or cut with a scalpel. Dried eggshells were fractured simply by breaking them with tweezers. Fractured whole eggs were also examined in order to have a picture of all the layers covering the oocyte.

Freeze-Fracturing

Purified chorions were cut in small pieces in distilled water and deposited on thin copper holders which were then rapidly quenched in liquid propane. The samples were fractured at −125°C with a liquid nitrogen-cooled knife in vacuum better than 10^{-6} Torr and replicated in a Balzers 301 freeze-etching unit. Freeze-etching was performed for 4 min. Half of the specimens were shadowed unidirectionally and the remainder were rotary shadowed (Margaritis *et al.,* 1977).

Metal evaporation was performed with electron bombardment guns using Pt–C electrodes. The Pt gun was set at a 35° angle to the specimen table surface, both for unidirectional and rotary shadowing. The C gun was set directly above the specimen table. The replicas were cleaned with sodium hypochlorite for half an hour, followed by a treatment with chromic acid overnight for some specimens, and, after distilled water washing, they were picked up on 400-mesh electron microscope grids. Electron microscopy was performed with a Philips EM301 microscope, operating at 60 or 80 kV. All electron micrographs for freeze-

FIG. 1. (A) A schematic diagram showing the development of various components of the eggshell (chorion) during the eight successive stages of oogenesis of *Salmo gairdneri* (fe, follicle cells; cre, cortex radiatus externus; cri, cortex radiatus internus; ca, cortical alveoli; yg, yolk granules; pv, pinocytic vesicles; hcv, hard core vesicles; yn, yolk nucleus; also see text). (B) Transmission electron micrograph of a thin section cut through a stage 2 *S. gairdneri* egg. Near the surface of the oocyte (OO) several infoldings (microvilli, MV) are seen and also numerous vesicles and organelles including hard core vesicles (hcv) and electron-lucent vesicles (LV) or else pinocytic vesicles (pv), mitochondria (M), and vesicular or tubular endoplasmic reticulum (ER). The cell membrane of the follicle cells (FE) is relatively smooth. No chorionic deposits can be discerned at this stage. Bar, 1 μm. (C–F) Transmission electron micrographs of thin sections cut through stages 3–6 *S. gairdneri* eggs, respectively. During stage 3 (C), osmiophilic homogeneous material is deposited at the bases of the microvilli (MV) of the oocyte. Several follicle cell (FE) protrusions (fcp) are in contact with the oocyte and might participate in the process. This material forms the outer part of chorion, cortex radiatus externus (CRE), which is deposited first. Bar, 1 μm. Choriogenesis (eggshell formation) continues at stage 4 (D) with the formation of the inner part of chorion, cortex radiatus internus (CRI). Newly synthesized and secreted, less osmiophilic, chorionic material is deposited between the oocyte microvilli. The eggshell has a columnar appearance at this stage. Bar, 1 μm. During stages 5 and 6 of choriogenesis (E and F), the CRI increases in thickness. Bar, 1 μm in both (E) and (F).

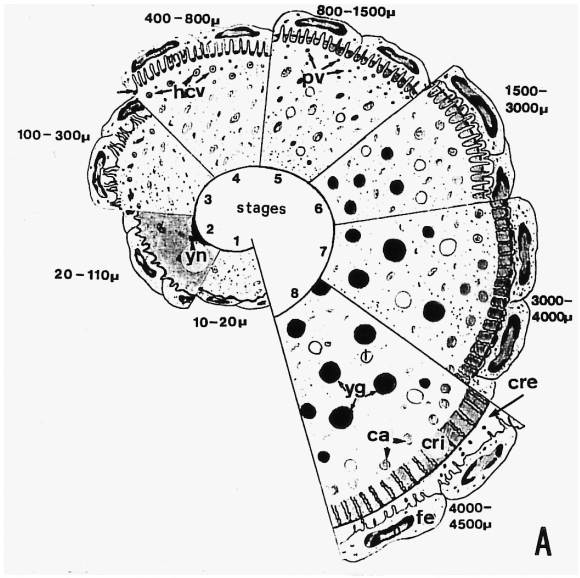
400 – 800µ
800–1500µ
hcv
pv
1500–
3000µ
100 – 300µ
stages
yn
20 – 110µ
10–20µ
3000–
4000µ
yg
cre
ca
cri
fe
4000–
4500µ
A

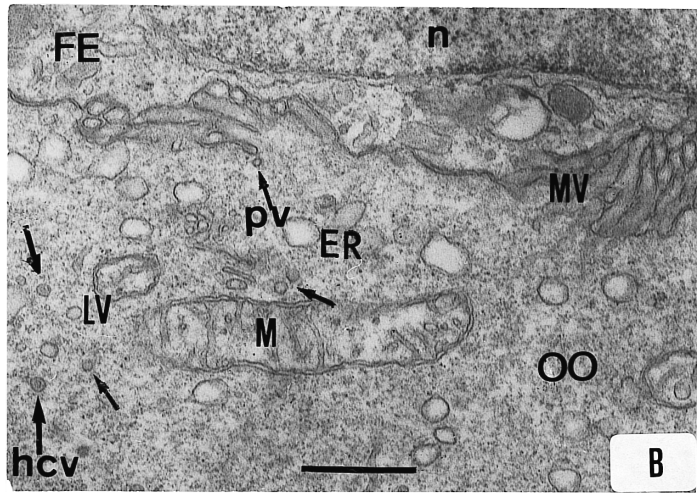
FE
n
MV
pv
ER
LV
M
OO
hcv
B

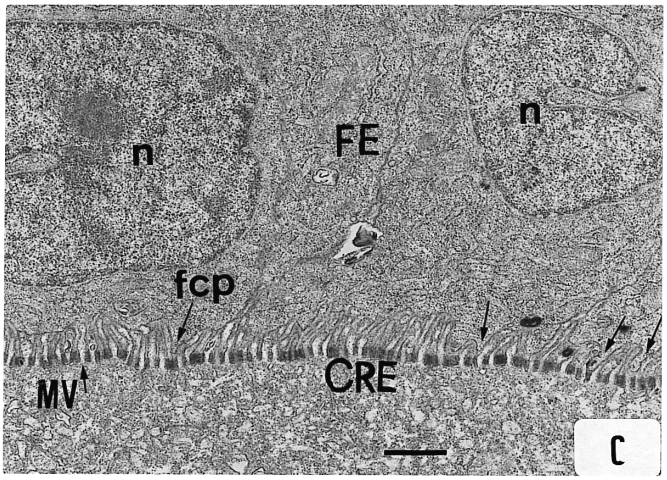
n
FE
n
fcp
MV
CRE
C

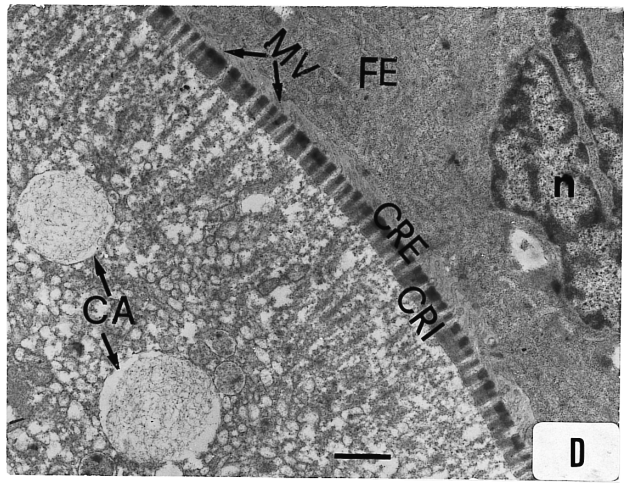
MV
FE
n
CRE
CRI
CA
D

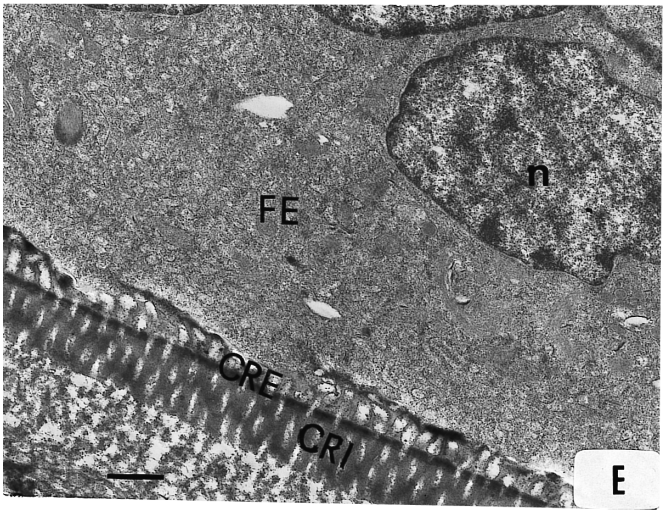
n
FE
CRE
CRI
E

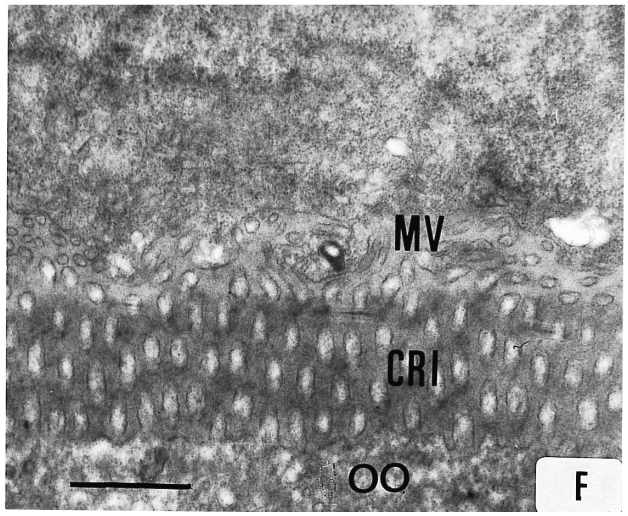
MV
CRI
OO
F

fracturing are positive images, i.e., platinum deposits appear dark.

Raman Spectroscopy

Eggs at different developmental stages were cut in half with fine scissors and washed several times in distilled water followed by 95% ethanol and sonication in water, to remove the oocyte, follicle cells, and other remnants. The eggshells were then thoroughly dried. The samples used for laser-Raman experiments were hemispherical half-eggshells. Raman spectra were measured on a Ramanor HG25 Jobin-Yvon spectrometer. The 514.5-nm line of a Spectra Physics 165 argon-ion laser, operating at 100 mW, was used for excitation. A 90° scattering geometry was employed, with the laser beam hitting the eggshell surface tangentially. Prolonged (2–4 hr) laser irradiation of the samples was necessary to reduce fluorescence and to measure reasonable Raman spectra. To further reduce the noise level, the spectra were recorded at a scanning speed of 10 cm^{-1}/min and a time constant of 2 sec. The spectral resolution was 5 cm^{-1}.

RESULTS

The formation of the eggshell has been studied by a combination of transmission and scanning electron microscopy at different developmental pre- and postovulatory stages.

Preovulatory Stages

Transmission electron microscopy data. The process of oogenesis in *S. gairdneri* has been divided into four types of follicles which make up eight distinct stages (Yamamoto *et al.,* 1965; van den Hurk and Peute, 1979). The previtellogenic follicles (10–300 μm in size), at which period the nucleus and cytoplasm are undergoing many changes, were divided into three stages. The vitellogenic follicles (400–3000 μm in size) were also subdivided into three stages: the stage of endogenous yolk formation, the stage of exogenous yolk formation, and the stage of yolk aggregation. In stage 7 (3000–4000 μm in size) the follicle is mature and it is ready to enter into the postovulatory stage. In the last stage (4000–4500 μm in size), the follicle is ruptured and the egg is expelled into the abdominal cavity of the fish.

Choriogenesis (eggshell formation) was subdivided by us into the same developmental stages to facilitate comparisons. Figure 1A shows the correspondence schematically. The first indication of chorionic material appears in stage 3 or the beginning of 4, following the formation of an extensive network of oocyte microvilli and follicular cell processes as well as the appearance of various vesicles in the oocyte. In stages 3 and 4 hard core vesicles (hcv) and pinocytic vesicles (pv) are observed as well as a large number of mitochondria, endoplasmic reticulum, and Golgi. In stage 5 the hard core vesicles disappear but the pinocytic vesicles are still present. In this stage, the inner eggshell (CRI), which is not as osmiophilic as the thin CRE layer, starts to be deposited.

In stage 6 the process of vitellogenesis approaches its end and the eggshell is almost fully formed. Finally, in stages 7 and 8 the follicular cell protrusions and the oocyte microvilli withdraw, leaving behind pore canals. These canals eventually close by plugs which consist of material similar in appearance to the remainder of CRE, in the CRE layer. At this final stage the egg has obtained a size of 4000–4500 μm in diameter and the eggshell a thickness of approximately 20–25 μm. Figures 1B–1F show stages 2–6 of choriogenesis, respectively. In stage 2 (Fig. 1B) the cell membrane of the follicle cells (FC) is relatively smooth and there are no chorionic deposits between the oocyte microvilli (MV).

Figure 1C is a transmission electron micrograph of a thin section cut through an early developing follicle in stage 3. At this stage the eggshell begins to form. The osmiophilic outer part of the eggshell CRE is the first layer to be deposited between the oocyte microvilli. It acquires a thickness of about 0.15 μm, which is constant throughout choriogenesis. The follicle cells are in close association at this stage and exhibit abundant granular endoplasmic reticulum, mitochondria, and electron-dense bodies. In the oocyte hard core vesicles are no longer observed.

The beginning of formation of the inner eggshell, CRI, is depicted in Fig. 1D. Both the oocyte and the follicle cells show intense pinocytic and protein synthesis activity. New, less osmiophilic, material is deposited underneath the CRE layer between the oocyte microvilli forming CRI. This results in a column-like appearance of the eggshell. Choriogenesis proceeds further in stages 5 and 6 (Figs. 1E and 1F). The column-like ultrastructure of the eggshell gradually disappears. Pore canals are kept in close

FIG. 2. (A) A diagram of a typical mature *S. gairdneri* follicle. Moving inward from the periphery the following layers can be seen: TH, theca layer; CF, collagen fibers; BM, basal membrane; FE, follicular epithelium; CRE; outer eggshell (cortex radiatus externus); CRI, inner eggshell (cortex radiatus internus); OO, oocyte (mv, microvilli; yg, yolk granules). (B–E) Scanning electron micrographs of preovulatory follicles at developmental stages 3–6, respectively. In (B), stage 3, only CRE has been formed. The different layers of the follicle are clearly seen (compare with A). Bar, 10 μm. In (C), stage 4, CRI has been formed, reaching a thickness of approximately 1.0 μm. Bar, 1 μm. In (D), stage 5, the thickness of CRI has increased to 1.8 μm, whereas in (E), stage 6, the oocyte microvilli penetrating the pore canals can be discerned. Bar, 1 μm in both (D) and (E). (F–G) (Stage 5) Scanning electron micrographs of the outer cortex radiatus internus surface of the eggshell after removal of cortex radiatus externus with 6 *M* urea extraction (F), and of the inner surface of the eggshell (G) without any treatment. The pore canals are seen in an almost regular hexagonal arrangement. Bar, 1 μm in both.

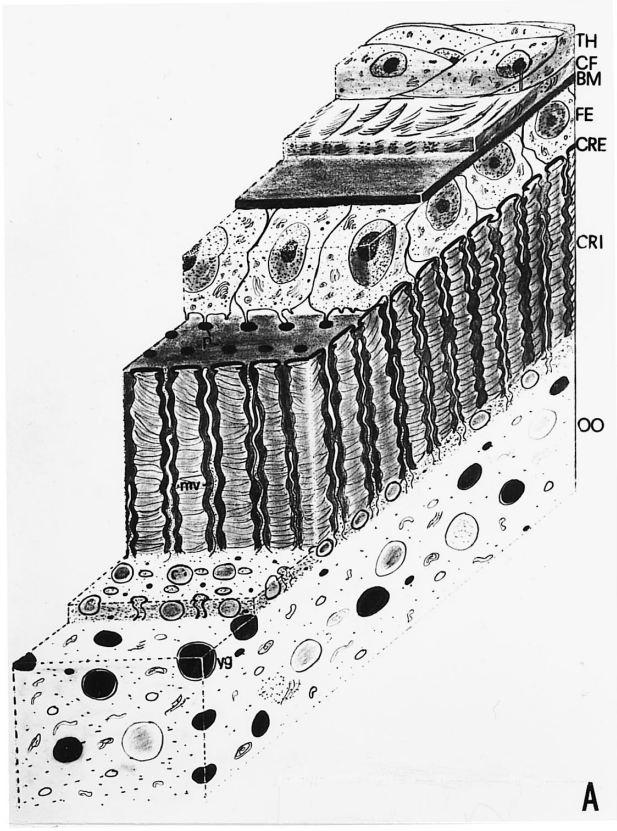
TH
CF
BM
FE
CRE
CRI
OO
mv
vg
A

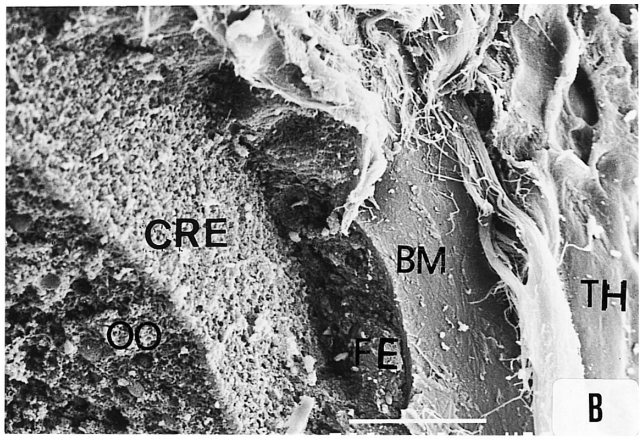
CRE
BM
TH
OO
FE
B

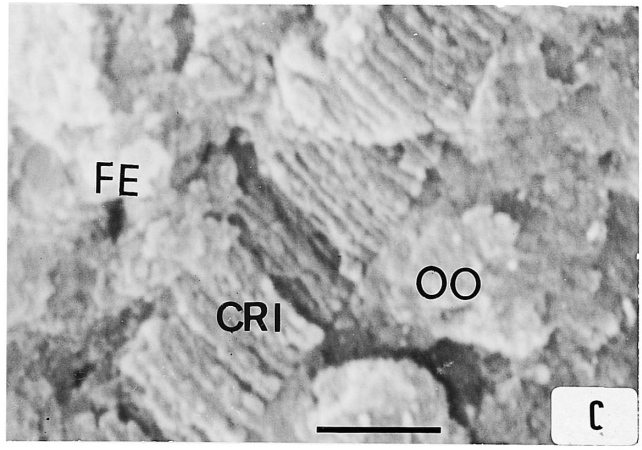
FE
OO
CRI
C

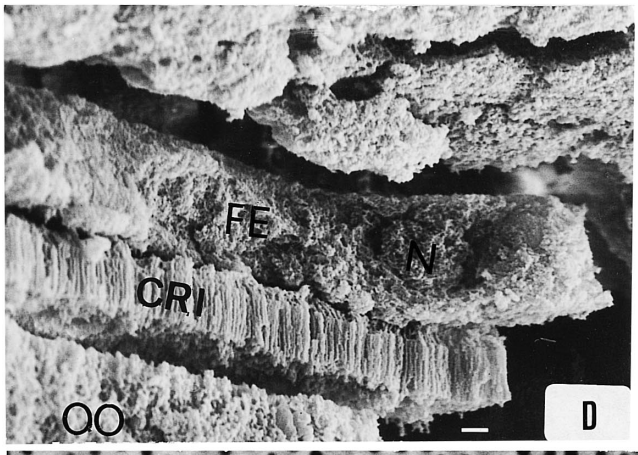
FE
N
CRI
OO
D

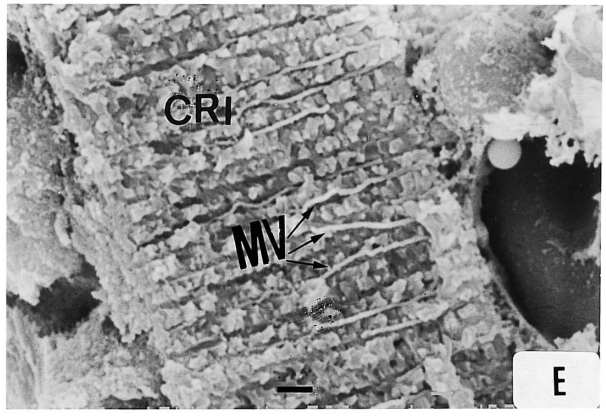
CRI
MV
E

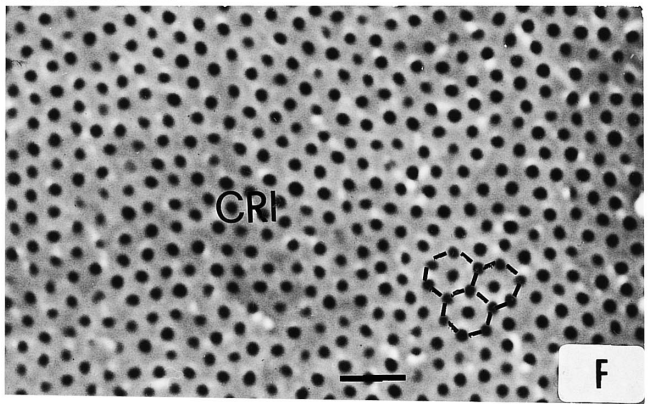
CRI
F

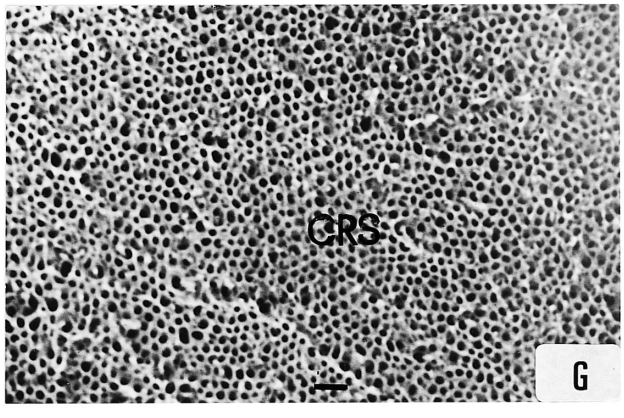
CRS
G

proximity to each other at these early developmental stages.

In preovulatory eggs near the end of choriogenesis (stage 7), the chorionic material is organized into lamellae around the oocyte microvilli, which traverse the pore canals (Figs. 3A–3C). Toward the end of stage 7 the process of choriogenesis terminates. The last material to be deposited are the plugs, which eventually close the outer opening of the pore canals (Fig. 3B). The follicle cell protrusions and the oocyte microvilli withdraw from the pore canals. The plug material appears to be of similar nature as the remainder of CRE, extending inward a few micrometers when plugs are fully formed (Fig. 3E).

Scanning electron microscopy data. A schematic block diagram of a developing *S. gairdneri* eggshell showing its relation to the oocyte, the follicle cells, and the other components of the follicular epithelium is presented in Fig. 2A, for clarity. Figures 2B–2G are scanning electron micrographs from preovulatory follicles at different, early, developmental stages, indicating significant changes of eggshell ultrastructure. The column-like ultrastructure of the early eggshell (Figs. 3B–3D) gradually changes into a lamellar architecture (Fig. 3E). Pore canals are arranged in a rather regular hexagonal fashion (Figs. 3F–3G), and the involvement of oocyte microvilli in their formation and organization is clear (Fig. 3C).

Postovulatory Stages

Transmission electron microscopy data. The *S. gairdneri* mature, postovulatory (stage 8) eggshell, ca. 20–25 μm thick, is a lamellar structure traversed by pore canals (Figs. 3D–3F). Lamellae are rather uniform in thickness. The pore canal shape in these and in micrographs taken from earlier developmental stages (Figs. 3B and 3C), indicates a helicoidal architecture for the eggshell (Grierson and Neville, 1981). Plugs close the outer openings of the pore canals (Figs. 3D and 3E). In some cases, the canals include oocyte microvilli remnants (Fig. 3F). At higher magnifications (data not shown) lamellae appear to have a homogeneous structure and there is no evidence for an underlying fibrillar ultrastructure. The lamellar structure is retained after fertilization (data not shown).

Scanning electron microscopy data. Figures 4A–4F are scanning electron micrographs taken from postovulatory isolated eggshells. Figures 4A, 4C, and 4E (stereomicrograph) were taken from cross-sectional rips of the eggshell at different orientations and help to visualize details of the internal eggshell lamellar architecture. The regular hexagonal arrangement of the pore canals on the outer smooth surface of CRI is shown in Fig. 4B. CRE together with the plugs of the pore canals have been removed after treatment with 6 *M* urea, followed by treatment with 1% mercaptoethanol. The three-dimensional picture of the eggshell is complete with Fig. 4D, which shows the inner surface of the eggshell (toward the oocyte). A rather complex network of interconnecting lamellae surrounds the pore canals. The micropyle, ca. 5 μm in diameter, situated in the animal pole of the egg, is seen in Fig. 4F. It is surrounded by a zone devoid of plugs and an outer region full of rather large plugs.

Fibrillar Ultrastructure of the Eggshell

In several fibrous helicoidal lamellar structures, the fibrillar ultrastructure cannot be discerned with transmission electron microscopy using classical methods of tissue embedding and staining (Grierson and Neville, 1981; Hamodrakas *et al.,* 1986). Two approaches were used in this study to circumvent the problem: (a) the eggshells were pretreated with thioglycollic acid, as described under Materials and Methods and (b) freeze-fracturing was used. Results are displayed in Fig. 5. The parabolic patterning of fibrils in oblique, thin sections of the eggshell (Figs. 5A–5C) indicates a helicoidal architecture (Bouligand, 1972), whereas a direct visualization of the

FIG. 3. (A–C) Transmission electron micrographs of thin sections cut through stage 7 *S. gairdneri* eggs. The eggshell has almost reached its final thickness. In sections tangential to the surface of the eggshell and to the oocyte, as in (A) and (C), the oocyte microvilli and the follicular cell processes are clearly seen inside the pore canals. This also holds for sections almost perpendicular to the surface of the eggshell (B). In the latter, it can be seen that the chorionic material is organized into lamellae which appear to be homogenous. The pore canals are orderly arranged in an almost regular hexagonal fashion (A and C). Their shape, in cross sections (A and C) and in longitudinal sections (B), suggests a helicoidal arrangement of the lamellae (Grierson and Neville, 1981). The CRE is perforated by the pore canals which are still open (A,B). Bar, 1 μm in all. (D,E,F) Transmission electron micrographs of thin transverse sections of mature isolated eggshells. The radial pore canals (PC) can be discerned in the lamellar CRI, with a characteristic twisted ribbon structure, implying a helicoidal architecture for the eggshell. The fibrous ultrastructure of the lamellae (L), however, cannot be discerned using classical methods of tissue embedding. The proteinaceous chorionic material appears to be homogeneous. The CRS layer is in close contact with the oocyte with no discrete boundary between it and the CRI (D). Therefore, it can be said with certainty that there is no such discrete layer in the *S. gairdneri* eggshell. The last material to be deposited are the plugs (P) in the outer openings of the pore canals on top of the oocyte microvilli, which also exhibit a helicoidal twist as can be seen in (F). The nature of the osmiophilic plug material is similar in appearance to the remainder of CRE (E). Bars, 10, 1, and 1 μm, respectively.

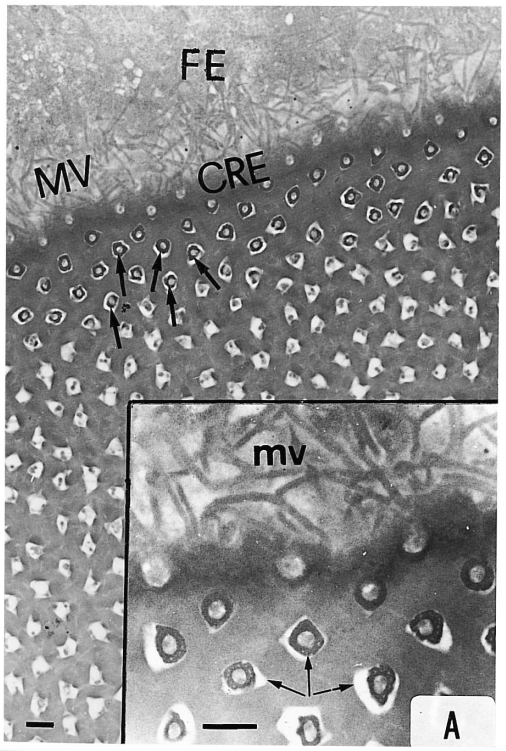
FE
MV
CRE
mv
A

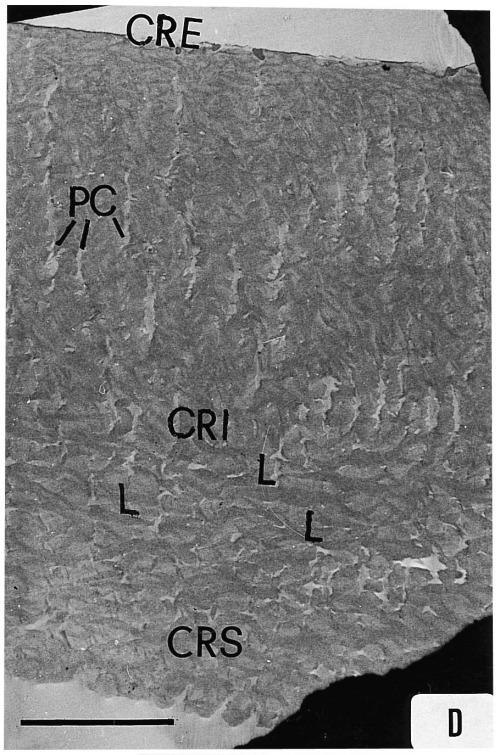
CRE
PC
CRI
L
L
L
CRS
D

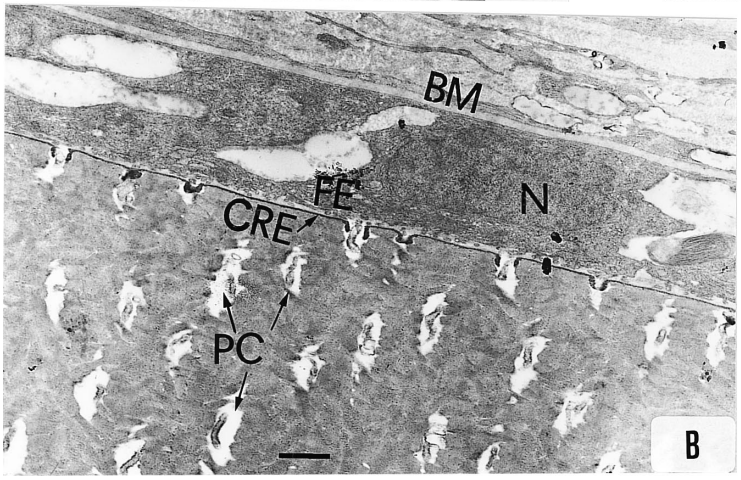
BM
FE
N
CRE
PC
B

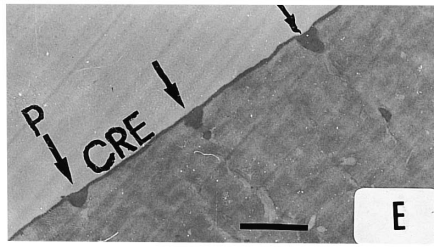
P
CRE
E

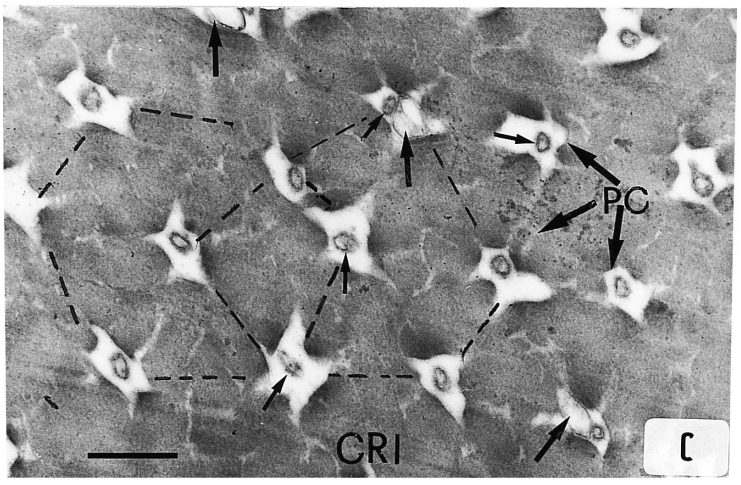
PC
CRI
C

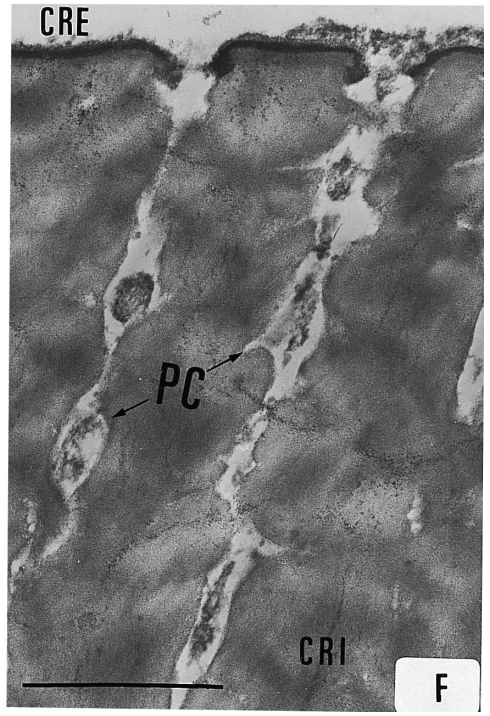
CRE
PC
CRI
F

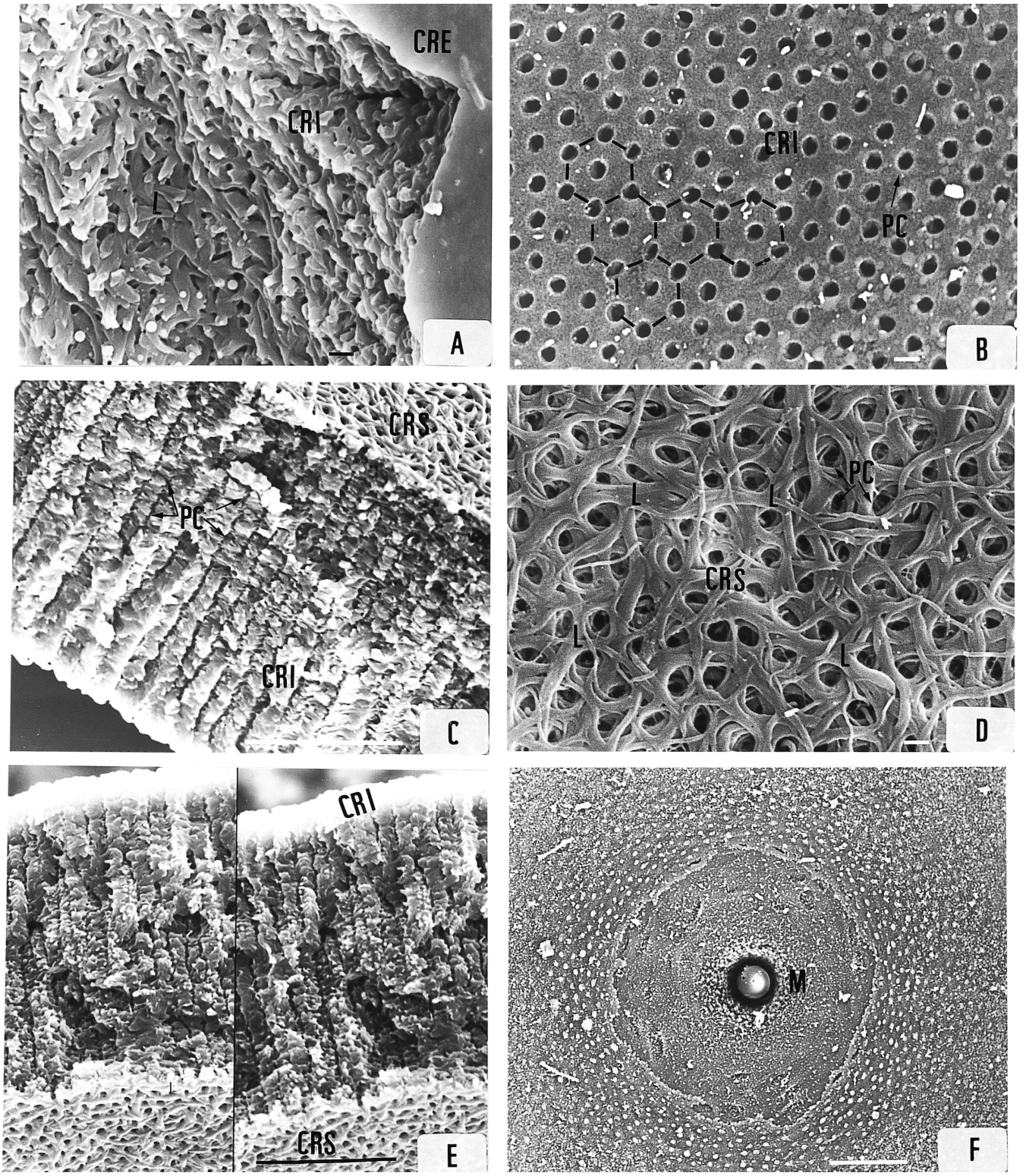

FIG. 4. Scanning electron micrographs from postovulatory eggs showing surface regions and interior architecture of the *S. gairdneri* eggshell: (A) An oblique cross-sectional rip through an eggshell showing a view of its lamellar organization (18 days after fertilization). Bar, 1 μm. (B) Extraction with 6 *M* urea removes CRE and the plugs, revealing an almost hexagonal arrangement of the pore canals. The pore canal distance is 1.3 μm and their diameter approximately 0.5 μm (2 days after fertilization). Bar, 1 μm. (C) A cross-sectional rip through the eggshell, almost perpendicular to its surface, reveals a different view of the lamellar organization of CRI. The pore canals are easily discerned traversing the eggshell. The thickness of the eggshell is approximately 21 μm (18 days after fertilization). Bar, 10 μm. (D) A view of the inner surface (CRS) of the eggshell. The network of lamellae, their interconnections and twist around the pore canals (PC) can be seen (18 days after fertilization). Bar, 1 μm. (E) A stereoscanning electron micrograph showing the pore canals (PC) traversing regularly arranged lamellae (18 days after fertilization). Bar, 10 μm. (F) The micropyle, 5.5 μm in diameter, is seen situated in the animal pole of the egg (2 days after fertilization). Bar, 10 μm.

helicoidal structure and of its constituent, 5- to 10-nm-thick fibrils was achieved after freeze-fracturing (Fig. 5D).

Raman Spectra

Our earlier work has shown that antiparallel β-pleated sheet structure predominates in the proteins of mature *S. gairdneri* eggshells (Hamodrakas *et al.,* 1987). In this study, an attempt was made to monitor possible changes of eggshell protein secondary structure during development.

According to extensive theoretical and experimental studies, the wavenumbers of amide I, II, and III bands in Raman spectra are useful indicators of protein and polypeptide secondary structure (Frushour and Koenig, 1975; Spiro and Gaber, 1977; Yu, 1977; Carey, 1982). The amide I bands (which occur in the region 1630–1690 cm^{-1}) have contributions from C-O stretching (approximately 70%) and C-N stretching (approximately 16%). The generally weak amide II Raman bands (1510–1570 cm^{-1}) and the amide III bands (1220–1330 cm^{-1}) have significant contributions from N-H in-plane bending and C-N stretching. Table I summarizes the diagnostic locations of these bands for α-helical, β-sheet, and β-turn structures and lists the corresponding wavenumbers observed in laser-Raman spectra of *S. gairdneri* eggshell samples.

Figure 6 shows laser-Raman spectra of *S. gairdneri* eggshells, from developmental stages 4 to 7 (Figs. 6A–6D, respectively). Table II gives the wavenumbers and our tentative assignments of the major bands appearing in the laser-Raman spectra. The bands at 1670 cm^{-1} (amide I) and 1230, 1240 cm^{-1} (amide III), which appear in all spectra, can be best interpreted as resulting from abundant antiparallel β-pleated-sheet structure (Hamodrakas *et al.,* 1987 and references therein). Therefore, it appears that antiparallel β-pleated-sheet structure is the predominant secondary structure of *S. gairdneri* eggshell proteins throughout development. This was confirmed by an analysis of the amide I band for all four spectra, following the method of Williams and Dunker (1981) as applied by Hamodrakas *et al.* (1984), to estimate the percentage of secondary structure of eggshell proteins. The results of the analysis are shown in Table III. For comparison, Table III also contains the results of the analysis of a laser-Raman spectrum (data not shown) taken from the eggshell of a fertilized egg. There seems to be little or no significant variation of the estimated secondary structure percentages at different developmental stages. This, perhaps, indicates that *S. gairdneri* eggshell proteins adopt and retain a defined structure during development. The distribution of the ϕ and ψ angles in the β-sheets appears to be rather narrow (the β-sheets exhibit a rather uniform structure), since the amide I band at ca. 1670 cm^{-1} is sharp: its half-width is approximately 40–50 cm^{-1}.

Raman spectra yield useful information on amino acid residues of Cys, Tyr, Phe, and Trp (Carey, 1982). Bands in the 500–550 cm^{-1} region are typically associated with the S-S stretching mode of the C-C-S-S-C-C structural unit of disulfide bonds. The bands at ca. 512 cm^{-1} in the Raman spectra of *S. gairdneri* eggshells may be assigned to S-S bridges in *gauche-gauche-gauche* (*g-g-g*) conformation (Sugeta *et al.,* 1972). There is no evidence for the existence of significant amounts of free sulfydryls, throughout development, as can be judged by the absence of bands in the 2530–2580 cm^{-1} spectral region, typically associated with the -SH stretching mode (Yu, 1977).

Tyrosines in *S. gairdneri* eggshell proteins appear to behave as hydrogen bond acceptors. This can be inferred from the intensity ratio of the tyrosine doublet at 850 and 830 cm^{-1} ($R = I_{850}/I_{830}$), which, in all four spectra was found to be between 1.0 and 2.2 (Hamodrakas, 1992, and references therein). Phenylalanine is also present in eggshell proteins, as seen from the intense peaks at 620 and 1035 cm^{-1} which are ascribable to Phe (Yu, 1977). The very intense and sharp band at 1003 cm^{-1} may also be attributed to Phe with a probable contribution from C_α-C′ and/or C_α-C_β stretching vibrations (Yu, 1977).

DISCUSSION

To our knowledge, this work is the first which presents a detailed picture of fish choriogenesis (eggshell development) in relation to the structure of eggshell proteins.

Laser-Raman spectroscopy is a very powerful and reliable technique for examining changes in the frequency of emitted radiation due to molecular vibrations (reviewed by Frushour and Koenig, 1975; Spiro and Gaber, 1977; Yu, 1977; Carey, 1982). It is related to, but distinct from, infrared spectroscopy, which examines absorption of radiation due to the same molecular vibrations. Both techniques have been empirically demonstrated to be quite sensitive to protein conformation. The weak emission as opposed to absorption of radiation by water is an important advantage of Raman spectroscopy for studies of biological materials.

The S. gairdneri eggshell is a relatively favorable structure for Raman spectroscopy studies. It consists almost exclusively of protein; thus, it meets the criterion of high protein density which is required for adequate sensitivity in Raman studies. The absence of major admixtures, such as chitin or other carbohydrates, minimizes interference from other

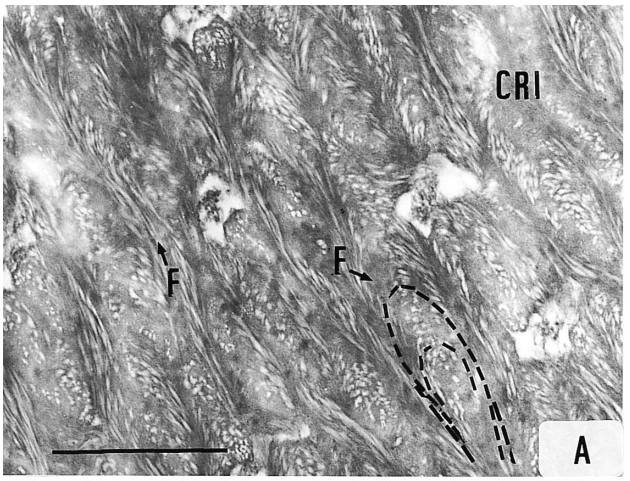
CRI
F
F
A

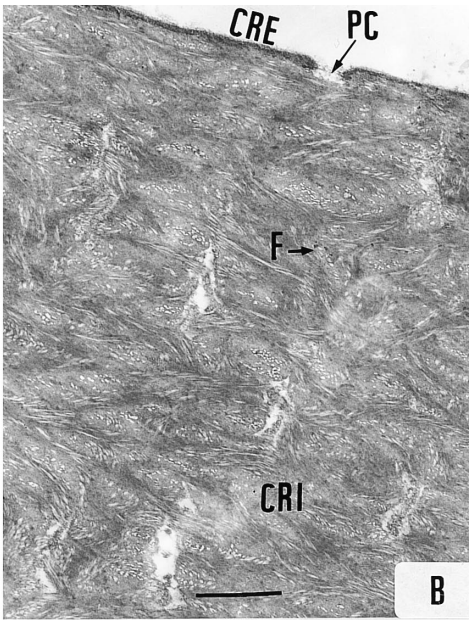
CRE
PC
F
CRI
B

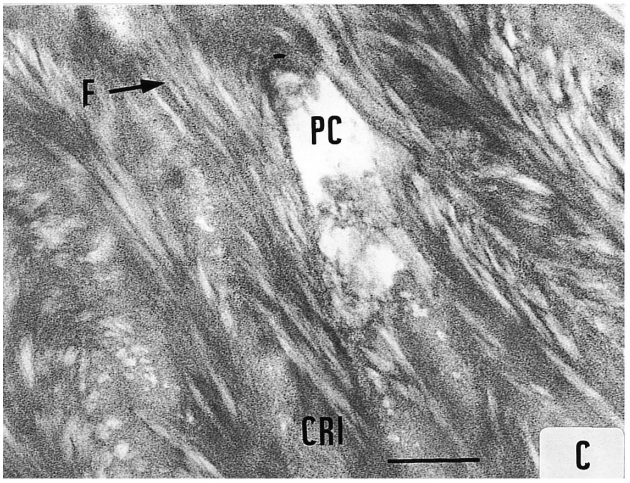
F
PC
CRI
C

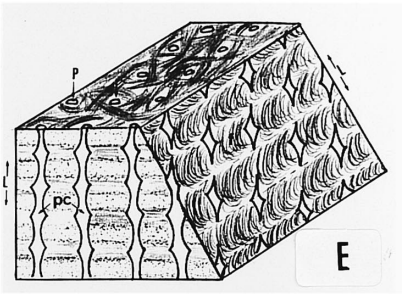
P
pc
E

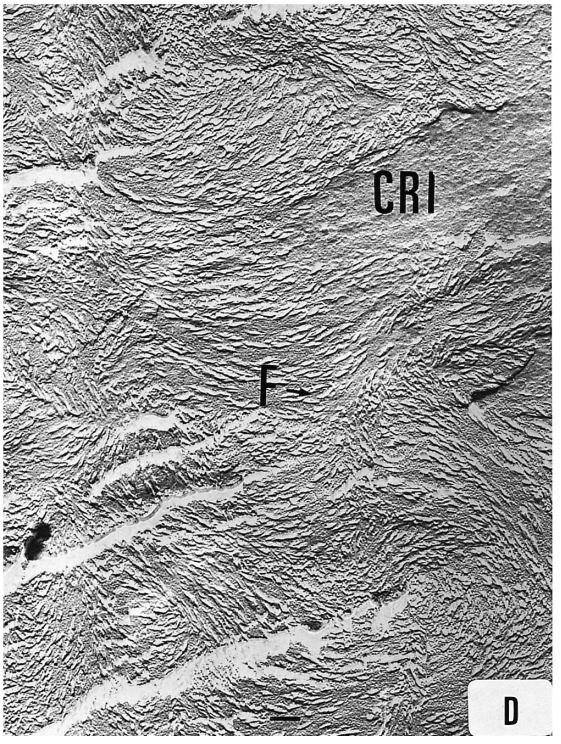
CRI
F
D

TABLE I

Summary of Diagnostic Amide Bands and Their Observation in *S. gairdneri* Eggshell[a]

Band nature	Bands characteristic of				Observed
	α-Helix	β-Sheet		β-Turn	
Amide I	1650–1660	1670–1680		1665, 1690	1670
Amide II	1516, 1545	1535, 1560	(I)	1550–55, 1567	1552
			(II)	1545, 1555, 1560	
Amide III	1260–1290	1230–1240		1290–1330	1240

[a] See, Frushour and Koenig, 1975; Spiro and Gaber, 1977; Yu, 1977; Carey, 1982.

than protein vibrations. Furthermore, we have encountered only limited interference from fluorescence in our studies. These features have permitted analysis of the intact eggshell protein structure, as opposed to protein extracts, ensuring that the structural features observed reflect a physiological state.

Our basic conclusion is that throughout choriogenesis antiparallel β-pleated-sheet structure is the prevalent secondary structure of *S. gairdneri* eggshell proteins. No major conformational changes of eggshell proteins appear to occur during development and the secondary structure remains uniform, dictating formation of higher-order (fibril) structure. These observations are in agreement with our proposal for the existence of a common molecular denominator, the antiparallel β-pleated-sheet structure, which dictates formation of helicoidal architecture in proteinaceous helicoidal eggshells (Hamodrakas, 1984).

According to previous investigations (Hagenmaier, 1973), *S. gairdneri* eggshell insolubility is accomplished after water activation or fertilization due to formation of isopeptide bonds involving the side chains of Glu and Lys or Arg residues of its constituent proteins. Apparently, an isopeptide bond forming enzyme, a transglutaminase, activated under these conditions, is responsible for eggshell insolubility, cross-linking eggshell proteins with mechanisms which remain obscure (Lonning *et al.,* 1984). Most probably, the enzyme is activated by Ca^{2+} ions. At different developmental stages, the eggshell of *S. gairdneri* was found to be in most cases only partially soluble in various solutions containing different combinations of denaturing and reducing agents, trying different pH and temperature conditions and also utilizing chemicals such as Na_2EDTA, which may inactivate the isopeptide bond forming enzyme (our data, not shown). Evidence from the laser-Raman experiments suggests that apart from the isopeptide bonds, which most probably are the major factors responsible for eggshell insolubility during development, disulfide bonds, present at all developmental stages, contribute to a certain extent.

The organization of *S. gairdneri* eggshell fibrils into a helicoidal architecture and details of fibril structure and packing were revealed after thioglycollic acid extraction and freeze-fracturing. Our experience in this and similar systems (Hamodrakas, 1992, and references therein) is that freeze-fracturing is the most reliable, artifact-free technique to unravel fibril structure and to permit direct visualization of helicoidal structure. Furthermore, it has the advantage of leaving the system chemically unmodified.

The intense oocyte and follicular epithelium activity, throughout choriogenesis, and the fact that oocyte microvilli and follicular cell protrusions appear to be involved in eggshell material secretion and deposition allow us to make the plausible assumption that both the oocyte and the follicular epithelium (follicle cells) contribute to the formation of the eggshell. This is in agreement with previous observations on this and several other fish species (Groot and Alderdice, 1984, and references therein). However, refined work is needed, perhaps with the help of autoradiographic experiments, to test this hypothesis.

FIG. 5. (A–C) Thioglycollic acid treatment (after Filshie and Rogers, 1962, and Grierson and Neville, 1981) reveals parabolic patterns of fibrils (F, dotted lines and arrows), in electron micrographs of oblique, thin sections cut through the eggshell of *S. gairdneri,* at different magnifications, implying a helicoidal architecture. The treatment removes the plugs from the pore canals (PC, arrow in B) leaving the remainder of CRE and CRI almost intact. Bars, 1, 1, and 0.3 μm. (D) Stereoscopic view of a Pt/C replica of a freeze-fracture plane within the eggshell of *S. gairdneri* (unidirectional shadowing) showing the structure of its constituent fibrils (F, arrow). The fracture has advanced across successive lamellae producing a series of steps. Therefore, the lamellar structure of the eggshell is clearly seen. The view also provides a direct visualization of the helicoidal architecture of the eggshell: the fibril orientation changes progressively from plane to plane. Bar, 0.3 μm. **(E)** Schematic drawing showing the helicoidal, lamellar (L) structure of *S. gairdneri* eggshell (after Grierson and Neville, 1981). Lamellae are traversed by pore canals (p, pc).

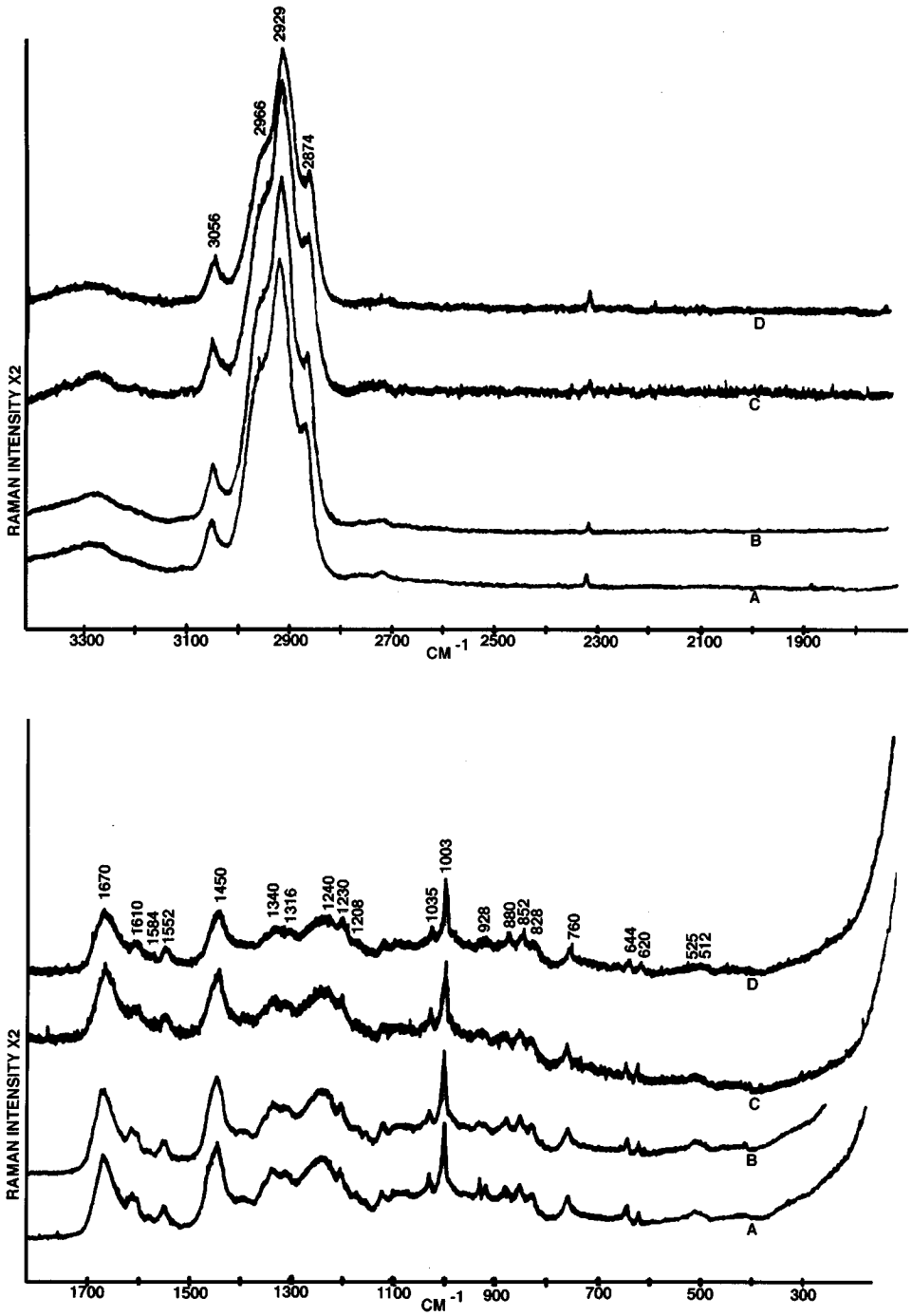

FIG. 6. Laser-Raman spectra obtained from four different developmental stages of the eggshell of *S. gairdneri* (A–D correspond to stages 4–7 respectively). A 90° scattering geometry was employed, with the laser beam hitting the eggshell surface tangentially. Instrumental conditions: excitation wavelength, 514.5 nm; scanning speed, 10 $cm^{-1} \cdot min^{-1}$; time constant, 2 sec; spectral resolution, 5 cm^{-1}; laser power at the sample, 100 mW.

TABLE II

Wavenumbers and Tentative Assignments of Bands in the Laser-Raman Spectra of the Eggshell of *S. gairdneri* (Fig. 6)

Wavenumber (cm^{-1})	Tentative assignment
512	S-S stretch
620	Phe
644	Tyr
760	C-S stretch? Trp?
828	Tyr
852	Tyr
880	Trp
1003(+)	Phe or C-c stretch
1208	Try, Phe
1230, 1240	Amide III (antiparallel β-sheet
1340	Amide III (β turns) or Trp
1450(+)	CH_2 deformation
1552	Amide II (β-turns) or Trp
1610	Try,Phe,Trp
1670(+)	Amide I (antiparallel β-sheet)
2800-3100(+)	C-H stretch

Note. (+) Denotes a strong peak.

There is perhaps a good reason why the helicoidal CRI is deposited between the nonhelicoidal CRE and the oocyte. Helicoidal monodomain structures need a constraining surface in order to be formed (Neville, 1988). The CRE layer may act as such. The helicoidal architecture of *S. gairdneri* eggshell and cross-linking of its constituent proteins via isopeptide and disulfide bonds seem to be particularly well suited for the eggshell to serve its primary role, that is, to withstand excessive mechanical pressures, protecting the oocyte and/or the developing embryo (Grierson and Neville, 1981).

We thank Dr. E. I. Kamitsos for his invaluable help with the laser-Raman experiments. P.P. and S.J.H. thank the Greek Ministry of Research and Technology for financial support.

TABLE III

Estimated Secondary Structure Percentages of *S. gairdneri* Eggshell Proteins from Analysis of the Amide I Band of Laser-Raman Spectra

	Percentage				
	A	B	C	D	E
α-Helix	2	0	12	29	0
Antiparallel β-sheet	53	62	59	37	56
Parallel β-sheet	0	0	0	0	0
β Turns	39	38	29	34	44
Unordered structure	7	0	0	0	0

Note. The method of Williams and Dunker (1981) was used as applied by Hamodrakas *et al.* (1984). A–D correspond to developmental stages 4–7, respectively, whereas E was derived from the spectrum of an eggshell from a fertilized egg.

REFERENCES

Anderson, E. (1967) The formation of the primary envelope during oocyte differentization in teleosts, *J. Cell Biol.* **35,** 193–212.

Bouligand, Y. (1972) Twisted fibrous arrangements in biological materials and cholesteric mesophases, *Tissue Cell* **4**(2), 189–217.

Carey, P. R. (1982) Biochemical Applications of Raman and Resonance Raman Spectroscopies, Academic Press, New York.

Filshie, B. K., and Rogers, G. E. (1962) An electron microscope study of the fine structure of feather keratin, *J. Cell Biol.* **13**, 1–12.

Filshie, B. K., and Smith, D. S. (1980) A proposed solution to a fine-structural puzzle, the organisation of gill cuticle in a crayfish (*panulirus*), *Tissue Cell* **12**(1)**,** 209–226.

Flugel, H. (1964) Electron microscopic investigations on the fine structure of the follicular cells and the zona radiata of trout oocytes during and after ovulation, *Naturwissenschaften* **51,** 564–565.

Flugel, H. (1967) Licht-und elektronenmikroskopiche Untersuchungen an Oozyten und Eiern einiger Knochenfische, *Z. Zellforsch. Mikrosk. Anat.* **83,** 82–116.

Frushour, B. J., and Koenig, J. L. (1975) Raman spectroscopy of proteins, *in* Clark, R. J. H., and Hester, R. E. (Eds.), Advances in Infrared and Raman Spectroscopy, Vol. I, pp. 35–97, Heyden, London.

Grierson, J. P., and Neville, A. C. (1981) Helicoidal architecture of fish eggshell, *Tissue Cell* **13**(4), 819–830.

Groot, E. P., and Alderdice, D. F. (1985) Fine structure of the external egg membrane of five species of Pacific Salmon and steelhead trout, *Can. J. Zool.* **63,** 552–566.

Hagenmaier, H. E. (1973) The hatching process in fish embryos. III. The structure, polysaccharide and protein cytochemistry of the chorion of the trout egg Salmo gairdneri (Rich.), *Acta Histochem.* **47,** 61–69.

Hamodrakas, S. J., Asher, S. A., Mazur, G. D., Regier, J. C., and Kafatos, F. C. (1982) Laser-Raman studies of protein conformation in the silkmoth chorion, *Biochim. Biophys. Acta* **703,** 216–222.

Hamodrakas, S. J. (1984) Twisted β-pleated sheet, the molecular conformation which possibly dictates the formation of the helicoidal architecture of several proteinaceous eggshells, *Int. J. Biol. Macromol.* **6,** 51–53.

Hamodrakas, S. J., Kamitsos, E. I., and Papanicolaou, A. (1984) Laser-Raman spectroscopic studies of the eggshell (chorion) of *Bombyx mori., Int. J. Biol. Macromol.* **5,** 149–153.

Hamodrakas, S. J., Margaritis, L. H., Papasideri, I., and Fowler, A. (1986) Fine structure of the silkmoth *Antheraea polyphemus* chorion as revealed by X-ray diffraction and freeze fracturing, *Int. J. Biol. Macromol.* **8,** 237–242.

Hamodrakas, S. J., Kamitsos, E. I., and Papadopoulou, P. G. (1987) Laser-Raman and infrared spectroscopic studies of protein conformation in the eggshell of the fish *Salmo gairdneri, Biochim. Biophys. Acta* **913,** 163–169.

Hamodrakas, S. J. (1992) Molecular architecture of helicoidal proteinaceous eggshells, *in* Case, S. T. (Ed.), Results and Problems in Cell Differentiation, Vol. 19, pp. 115–186, Springer-Verlag, BerlinHeidelberg.

Hurley, D. A., and Fischer, K. C. (1966) The structure and development of the external membrane in young eggs of the brook trout *Salvelinus fontinallys* (*Mitschill*), *Can. J. Zool.* **44,** 173–190.

Laale, H. W. (1980) The perivitelline space and egg envelopes of bony fishes: A review, *Copeia* 210–226.

Lonning, S., Kjorsvik, E., and Davenport, J. (1984) The hardening process of the egg chorion of the cod, *Gadus morhua L.,* and lumpsucker, *Cyclopterus lumpus L., J. Fish Biol.* **24,** 505–522.

Margaritis, L. H., Elgsaeter, A., and Branton, D. (1977) Rotary replication for freeze-etching, *J. Cell Biol.* **72,** 47–56.

Mazur, G. D., Regier, J. C., and Kafatos, F. C. (1982) Order and defects in the silkmoth chorion, a biological analogue of a cholesteric liquid crystal, *in* Akai, H., and King, R. C. (Eds.), Insect Ultrastructure, Vol. I, pp. 150–183, Plenum, New York.

Neville, A. C. (1988) The need for a constraining layer in the formation of monodomain helicoids in a wide range of biological structures, *Tissue Cell* **20**(1), 133–143.

Orfanidou, C. C., Hamodrakas, S. J., Margaritis, L. H., Galanopoulos, V. K., Dedieu, J. C., and Gulik-Krzywicki, T. (1992) Fine structure of the chorion of *Manduca sexta* and *Sesamia nonagrioides* as revealed by scanning electron microscopy and freeze-fracturing, *Tissue Cell* **24**(5), 735–744.

Orfanidou, C. C., Hamodrakas, S. J., Chryssikos, G. D., Kamitsos, E. I., Wellman, S. E., and Case, S. T. (1995) Spectroscopic studies of *Manduca sexta* and *Sesamia nonagrioides* protein structure, *Int. J. Biol. Macromol.* **17**(2), 93–98.

Spiro, T. G., and Gaber, B. P. (1977) Laser-Raman scattering as a probe of protein structure, *Annu. Rev. Biochem.* **46,** 553–572.

Sugeta, H., Go, A., and Miyazawa, T. (1972) S-S and C-S stretching vibrations and molecular conformations of dialkyl disulphides and cystine, *Chem. Lett.* **1,** 83–86.

van den Hurk, R., and Peute, J. (1979) Cyclic changes in the ovary of the rainbow trout *Salmo gairdneri,* with special reference to sites of steroidogenesis, *Cell Tissue Res.* **199,** 289–306.

Williams, R. W., and Dunker, A. K. (1981) Determination of the secondary structure of proteins from the amide I band of the laser-Raman spectrum, *J. Mol. Biol.* **152,** 783–813.

Yamamoto, K., Oota, I., Takano, K., and Ishikawa, T. (1965) Studies on the maturation process of the rainbow trout, *Salmo gairdneri irideus.* I. Maturation of the ovary of a one-year old fish, *Bull. Jpn. Soc. Sci. Fish* **31,** 123–132.

Yu, N. T. (1977) Raman spectroscopy: A conformational probe in biochemistry, *CRC Crit. Rev. Biochem.* **4,** 229–280.